Outer Membrane Phospholipase A Dimer Stability Does Not Correlate to Occluded Surface Area[†]

Alexandra Ebie Tan and Karen G. Fleming*

T. C. Jenkins Department of Biophysics, Johns Hopkins University, 3400 North Charles Street, Baltimore, Maryland 21218

Received July 31, 2008; Revised Manuscript Received September 23, 2008

ABSTRACT: Despite the key roles of oligomeric membrane proteins (MPs) in many known cellular pathways, the principles governing their oligomer stability are not well-understood. Previous work with the α-helical MPs bacteriorhodopsin (bR) and glycophorin A (GpA) shows that lost buried surface area linearly correlated with perturbations in protein stability. Although this is a significant discovery, the predictive power of this correlation is limited by the data. Because both bR and GpA have α-helical secondary structural motifs, it is unclear whether this correlation would be observed for MPs with a β-barrel motif. We addressed this question by measuring the thermodynamic consequences of interfacial amino acid changes at the dimer interface of β-barrel MP outer membrane phospholipase A (OMPLA). We created sequence variants to reduce the contact surface area of the OMPLA dimer interface by introducing single-alanine substitutions and used sedimentation equilibrium analytical ultracentrifugation to determine the dimerization free energies for these variants. The integrity of each variant was verified by two functional assays: specific activity and resistance to thermal denaturation, which showed that structural changes were restricted to the local environment. Using this information, we calculated the anticipated packing defects due to side chain deletion and compared this to the free energy perturbations for each residue. Contrary to the findings with bR and GpA, our study found no correlation between the contact surface area lost and the perturbations to OMPLA dimer stability. We conclude that van der Waals packing may not be a strong predictor of stability for all membrane proteins.

Our understanding of membrane protein stability is substantially limited by the lack of data addressing this scientific problem. Despite the significant strides that have been made, it is still unknown how structural and thermodynamic forces stabilize and modulate membrane proteins. Some evidence suggests polar residues play an essential role in stabilizing the tertiary and quaternary structures of membrane proteins (*1*−*5*). Although the introduction of a polar residue into the hydrophobic environment of the membrane may be energetically unfavorable, the low dielectric constant of the membrane causes satisfied hydrogen bonding pairs to have a significant stabilizing effect (*1*). Other data contrary to this idea suggest that polar residues are relatively rare in membrane proteins, and hydrogen bonds play only a small and localized role in membrane protein stability (*6*). Instead, it has been argued that van der Waals interactions are the dominant driving force for structural stability (*7*−*10*). Two studies by Doura et al. and Faham et al. give intriguing evidence that suggests a direct correlation between the extent of side chain packing of aliphatic residues and their free energy contributions to stability (*7, 8*). Both studies used α-helical membrane proteins as a model system, so broad implications can be hypothesized only for other membrane proteins; whether this correlation can predict stability perturbations in β-barrel membrane proteins remains unknown. The goal of this study was to explore whether loss of packing interactions could predict perturbations to oligomer stability for membrane proteins with a β-barrel motif.

To address this question, we constructed variants of membrane protein β-barrel outer membrane phospholipase A (OMPLA)[1] with predicted packing defects at the dimer interface. The X-ray crystal structures of both monomeric (PDB entry 1QD5) and dimeric (PDB entry 1QD6) forms of OMPLA showed that the dimer is formed by a rigid-body docking of the two monomers. We previously showed that two effector molecules, a lipid substrate and calcium cofactor, promote dimerization of OMPLA in detergent micelles by binding along the dimer interface (*11*). Here we use sedimentation equilibrium to determine the energetic packing contributions of side chain residues that make intermonomer contacts at the dimer interface.

OMPLA is a particularly good candidate for these studies because it is an enzyme, and its function requires precise dimer interface architecture for efficient substrate cleavage (*12, 13*). Therefore, specific activity can be used to detect whether any of the packing variants introduce structural changes that extend beyond the local side chain environment. Additionally, we verified the structural integrity of each variant using resistance to thermal denaturation. Although this assay does not yield the free energy of folding, it can

[†] This work is supported by NSF Grant MCB0423807.

* To whom correspondence should be addressed. Phone: (410) 516-7256. Fax: (410) 516-4118. E-mail: Karen.Fleming@jhu.edu.

[1] Abbreviations: bR, bacteriorhodopsin; BSA, buried surface area; GpA, glycophorin A; HSF, hexadecylsulfonyl fluoride; MP, membrane protein; OMPLA, outer membrane phospholipase A; OSA, occluded surface area; SE-AUC, sedimentation equilibrium analytical ultracentrifugation; PDB, Protein Data Bank.

10.1021/bi801436a CCC: $40.75
Published on Web 10/22/2008

Table 1: OMPLA Residues Ranked by Intersubunit Occluded Surface Area (OSA)[a]

ranking	residue	intersubunit OSA (Å^2)
1	L32	48.51
2	H234	28.85
3	S148	28.23
4	F109	24.78
5	F30	23.93
10	L71	17.11
14	L73	15.51
20	Q94	10.75
39	T112	2.10
41	E25	1.38

[a] After the OSA for each residue was calculated, the residues were ranked by decreasing intersubunit OSA. The five residues with the greatest individual intersubunit OSA are shown along with three residues (L71, Q94, and L73) highlighted in the literature and two low-intersubunit OSA residues (E25 and T112) selected as controls in this study.

indicate whether the apparent stabilities of the variants greatly differ from that of the wild-type protein.

MATERIALS AND METHODS

Determination of Variant Structures for OSA and BSA Calculations. To allow for direct comparison of our results for OMPLA with previous studies, we emulated the methods used in the correlation studies by Doura (*7*) relating to occluded surface area (OSA) and Faham (*8*) relating to buried surface area (BSA). For this reason, the structures used to determine lost OSA and lost BSA were determined differently.

For OSA calculations, point mutation variants were automatically obtained using the "mutate" function available in WHAT IF starting with the wild-type dimer crystal structure (PDB entry 1QD6) (*12*) with HSF and calcium coordinates excluded. To allow for possible side chain rearrangements resulting from alanine substitutions, variant structures were allowed to rearrange using the "deball" command in WHAT IF. No backbone rearrangements were allowed. This debumping command was repeated five times on all structures. HSF and calcium coordinates were then added back to the final minimized structures. OSA calculations indicated no significant steric clash resulted from adding effector molecules after protein rearrangements were allowed.

For BSA calculations, variant structures were determined by deleting side chain coordinates from the wild-type dimer crystal structures (PDB entry 1QD6), leaving only the β-carbon and backbone residue coordinates the same to reflect each individual alanine substitution.

Occluded Surface Calculation. The occluded surface area calculation program was used to determine the occluded surface for each residue based on the OMPLA dimer crystals determined for the wild-type and each variant as described in the previous section. In this calculation, a ray length of 2.8 Å was used to extend out perpendicular from each monomer molecular surface. Intermolecular contacts with the van der Waals surface of the adjacent monomer were calculated. To identify promising candidates for this study, occluded surface area was initially determined individually for each residue in the wild-type crystal structure (PDB entry 1QD6) (Table 1). For comparison to experimental values, the occluded surface area was calculated for each variant using minimized variant structures as described in the previous section and subtracted from the value determined for the wild-type protein, resulting in the overall loss of OSA as a consequence of mutagenesis. The calculated values for the expected occluded surface area lost for each variant dimer are included in Table 2.

Table 2: Calculated Losses of Occluded Surface Area, Calculated Losses of Buried Surface Area, and Experimentally Determined Free Energies of Association for Each Variant[a]

ranking	variant	calculated loss of OSA (Å^2)	calculated loss of BSA (Å^2)	SE-AUC-determined ΔG_{app} (kcal/mol)
1	L32A	90.34	71.27	−8.23 ± 0.25
2	H234A	86.53	199.33	−8.86 ± 0.25
3	S148A	6.34	22.28	−8.91 ± 0.24
4	F109A	86.30	23.25	−6.70 ± 0.38
5	F30A	30.25	−294.23	−8.21 ± 0.14
10	L71A	60.79	62.47	−7.43 ± 0.24
14	L73A	38.72	58.49	−8.22 ± 0.25
20	Q94A	31.87	21.47	−7.99 ± 0.38
39	T112A	5.23	−2.85	−8.57 ± 0.19
41	E25A	20.66	54.72	−8.15 ± 0.08

[a] The loss of occluded surface area for each variant is the sum of the total occluded surface area (OSA) determined for the minimized wild-type dimer minus the sum of the total occluded surface area calculated for each minimized variant structure. The loss of buried surface area (BSA) is the total buried surface area calculated for the wild-type minus the buried surface area calculated for each variant as described in Materials and Methods. The experimentally determined free energy of association (ΔG_{app}) values for each variant were obtained by SE-AUC and are represented graphically in Figures 2 and 3.

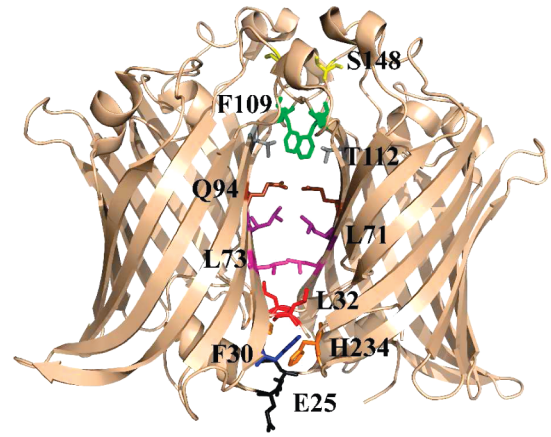

FIGURE 1: Interface packing variants. The positions of the 10 interface packing residues selected for alanine mutagenesis are shown as sticks on the ribbon form of the OMPLA dimer backbone structure (PDB entry 1QD6). The calcium cofactor and HSF molecules included in the wild-type structure are not shown.

Buried Surface Area Calculation. The buried surface areas of the wild-type structure and each of the variants were determined as previously described. The attenuated dimer structures were also used to construct both a "monomer 1" and "monomer 2" structure. The accessible surface area calculation for each of the monomers alone and the dimer for each variant was performed with MSROLL (*14*) with a 1.4 Å probe radius. The buried surface area is the difference between the sum of the monomer accessible surface areas and that of the dimer. The change in buried surface area for each variant was then determined by subtracting the buried surface area of the variant from the wild-type value. The calculated values for the expected loss of buried surface area are included in Table 2.

Cloning and Expression. Sequence variants were generated using the Strategene Quikchange protocol with appropriate

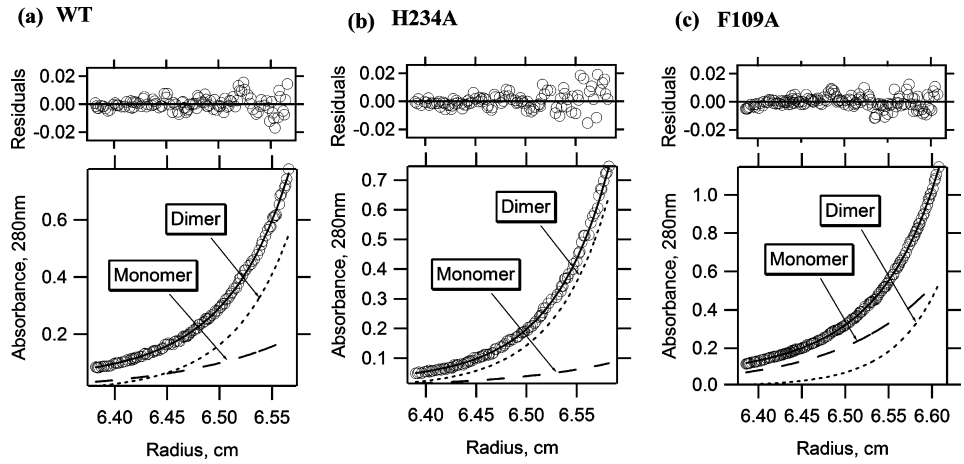

FIGURE 2: Representative radial distributions from sedimentation equilibrium analytical ultracentrifugation data for (a) the wild-type, (b) H234A, and (c) F109A fit to a monomer−dimer model. The data shown were collected in buffer with 2.5 mM C14-SB and an initial protein concentration of 6.6 μM. Empty circles show the data, and the global fit for each model is indicated by the solid line. The calculated monomer and dimer species distributions derived from self-associating fits are indicated by the dashed and dotted lines, respectively. The top panels are residuals indicating the difference between the data and the fit at each point.

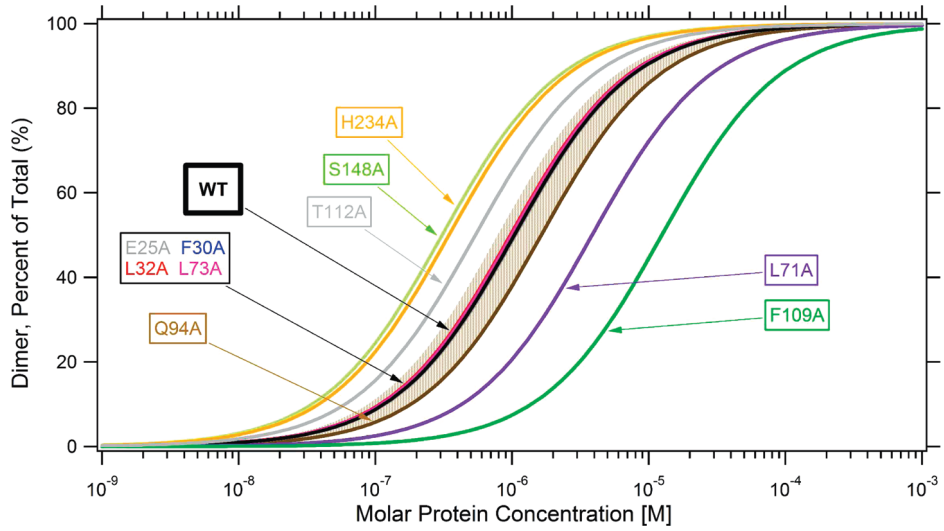

FIGURE 3: Comparison of the dimer species equilibrium distribution of interfacial packing variants. The percent dimer is given as a function of molar protein concentration. Population distributions are calculated using experimentally determined ΔG_{app} values for sulfonylated variants in the presence of calcium at 2.5 mM C14-SB. The shaded area denotes the range of values determined to be insignificant from that of the wild-type by a Student's t test ($p < 0.05$). Variants can be divided into three categories: wild-type-like dimerization (WT, L32A, F30A, Q94A, L73A, and E25A), more stable than the wild-type (S148A, T112A, and H234A), and less stable than the wild-type (L71A and F109A).

primers and then confirmed by sequencing. Both wild-type OMPLA and the interface variants were expressed and refolded as described previously (*11*). Refolded OMPLA was subsequently exchanged into C14-SB detergent (Sigma) and purified using a diethylaminoethyl (DEAE) Fast Flow Sepharose column followed by separation of the folded protein fraction using a FPLC system Q6 column (Bio-Rad) as described previously (*11*). Folded fraction was eluted between 260 and 320 mM KCl.

HSF Labeling of OMPLA. Hexadecylsulfonyl fluoride (HSF) was synthesized and structurally verified by NMR as described previously (*15, 16*). Purified wild-type OMPLA and variants were reacted with HSF and incubated overnight at room temperature as described previously (*11, 17, 18*).

Using both the colorimetric substrate 2-hexadecanoylthio-1-ethylphosphorylcholine (HEPC, Cayman Chemicals) and 5′-dithiobis(2-nitrobenzoic acid) (DTNB), the phospholipase activity of labeled OMPLA was monitored as described by the activity assay which follows (*17*). HSF irreversibly modifies the catalytic site serine at position 144, leading to inactivation of OMPLA. A loss of activity of the HSF-labeled protein indicates modification of the substrate binding site by HSF. We can, therefore, ensure a homogeneous population of labeled protein by comparing the phospholipase activity of the HSF-labeled protein to that of the unlabeled protein. Samples showing a >98% loss of activity are considered completely labeled. For the activity assay protocol, see below.

Sedimentation Equilibrium Analytical Ultracentrifugation. Immediately before sedimentation equilibrium analysis, purified OMPLA variants were exchanged by ion-exchange chromatography into C14-SB detergent micelles as described previously (*9, 11*) with EPPS (pH 8.3) substituted for Tris-HCl (pH 8.3). Sedimentation equilibrium experiments were conducted with a Beckman XL-A analytical ultracentrifuge in six-sector cells according to previously published protocols (*9, 11*). The absorbance at 280 nm was measured for three initial protein concentrations (3.3, 6.6, and 10.0

μM) and three rotor speeds (16300, 20000, and 24500 rpm) in a solution of 20 mM EPPS (pH 8.3), 200 mM KCl, 10 mM $CaCl_2$, and 2.5 mM C14-SB. The mass contribution of the detergent was offset by density matching the detergent to the buffer with 13% deuterium oxide. WINMATCH was used to verify that equilibrium was reached at each speed. Sedimentation equilibrium profiles were analyzed using the Windows version of NONLIN (*19*).

Specific Activity Assay. The specific activity of wild-type OMPLA and each variant was determined using the colorimetric substrate 2-hexadecanoylthio-1-ethylphosphorylcholine (HEPC, Cayman Chemicals) and 5′-dithiobis(2-nitrobenzoic acid) (DTNB) to monitor the phospholipase activity as described previously (*17*). Protein was incubated overnight at room temperature at a final protein concentration of 0.2 mg/mL in buffer containing 20 mM EPPS (pH 8.3), 200 mM KCl, 2.5 mM C14-SB, and 2 mM EDTA. The final assay buffer contained 50 mM EPPS (pH 8.3), 20 mM $CaCl_2$, 1 mM HEPC, 0.8 mM DTNB, and 2.5 mM C12-SB. The absorbance at 412 nm of 0.2 μg of OMPLA was monitored for 6 min. The specific activity was calculated on the basis of data collected after the first 30 s of the assay as described previously (*17*). The reported activity is an average of three independent assay measurements.

Thermal Denaturation. Protein samples used for activity assay were also used in the thermal denaturation assay. Samples were quenched by adding 5× SDS loading buffer to a final concentration of 0.5× SDS−PAGE loading buffer. Samples were heated to 80 °C in an MJ Research PTC-200 thermal cyler for 10 min and analyzed via densitometry of SDS−PAGE analysis as previously described (*17*). To ensure the percentage unfolded protein reported only on the amount of protein unfolded due to thermal denaturation, control samples which were quenched with SDS buffer but not thermally denatured were also analyzed by densitometry to determine the amount of protein unfolded prior to thermal denaturation. Twenty-six of the 33 samples exhibited no detectable amount of unfolded protein. The remaining seven exhibited no more than 5% unfolded protein before thermal denaturation. For these samples, the data were adjusted to show protein unfolded only as a result of thermal denaturation.

Student's t Test. Student's *t* test analysis was used to determine whether variants differed significantly from the wild-type. This method was used to analyze sedimentation analytical ultracentrifugation data, activity assay data, and thermal denaturation data. To calculate the *t* value, we used the following equation:

$$\frac{\bar{\chi}_1 - \bar{\chi}_2}{\left(\sqrt{\frac{s_1^2 + s_2^2}{n}}\right)}$$

where $\bar{\chi}_1$ denotes the average wild-type value, $\bar{\chi}_2$ denotes the average variant value, s_1 is the standard deviation for the wild-type values, s_2 is the standard deviation calculated from the variant values, and n is the number of participants in each group. In the activity assay and thermal denaturation experiments, three independent values were collected; thus, $n = 3$ in all statistical analyses. Each individual sedimentation equilibrium analytical ultracentrifugation (SE-AUC) experiment consisted of nine globally fit radial distributions. The wild-type and each variant experiment was repeated a total of six times. Thus, the n value in the statistical evaluation of the SE-AUC data was 6. The resulting *t* value was compared to *p* value distribution charts for a two-tailed distribution using a probability of 0.05 and a degree of freedom equal to the total number of participants in both groups minus 2. Variant values were considered statistically significant from the wild-type value if the calculated *t* value was above that given by the chart.

RESULTS

Packing Variants Exhibit a Range of Perturbations on Dimerization. To select the interfacial residues with the large occluded surface area, the intramolecular occluded surface area (OSA) was calculated for each residue from the crystal structure of dimeric wild-type OMPLA (PDB entry 1QD6) using the occluded surface area calculation program first introduced by Fleming et al. (*20*). Residues were ranked in decreasing order on the basis of the resulting OSA. The five residues with the greatest OSA (L32, H234, S148, F109, and F30) were selected for alanine mutagenesis (Table 1). Since specific activity was used as a reporter of interface structural integrity, the residues known to be involved in the catalytic activity as well as calcium binding were not considered for mutagenesis. Thus, any changes in activity would not be a result of direct active site perturbations. As a control, two residues with negligible OSA contributions were also selected, T112 and E25, which ranked 39th and 41st, respectively. Some residues from our list were studied previously by Kingma and colleagues (*21*), who found that Q94A as well as the triple mutant L32A/L71A/L73A (L32, first on our list) showed loss of calcium affinity and loss of dimerization, as assessed by glutaraldehyde cross-linking. Interestingly, under the same conditions, an F109M variant (F109, fourth on our list) exhibited wild-type calcium activity as well as wild-type dimerization in the presence of calcium. To determine if these variants affect dimerization because of lost occluded surface area, we included residues L71, L73, and Q94 in our study, ranking 10th, 14th, and 20th, respectively, in their OSA. Table 1 lists the calculated intersubunit occluded surface area for the 10 selected residues, as calculated for each residue from the OMPLA dimer crystal structure. Figure 1 shows the location of each residue on the dimer interface in the wild-type structure.

Perturbations to dimer stability were measured using sedimentation equilibrium analytical ultracentrifugation (SE-AUC) in the presence of the cofactor calcium and the covalently bound substrate analogue HSF (*11*). Since SE-AUC is a direct measure of mass, it can report on both molecular weights and equilibrium constants of membrane protein species associating within detergent micelles (*7, 9*−*11, 17, 19, 22*−*26*). To determine the oligomeric distribution of each OMPLA variant, the radial distribution profiles of nine equilibrium data sets (three initial protein concentrations at three speeds) were globally fit using a nonlinear least-squares curve fitting procedure, NONLIN, that incorporates the equations describing sedimentation equilibrium (*27*). Panels a−c of Figure 2 show representative radial distribution plots for the wild-type protein and two variants at an initial protein concentration of 6.6 μM and 20000 rpm. The empty circles are the raw data, which are fit to the model represented by the solid line. In all cases, the data were best described by

a monomer−dimer model (Supporting Information), which is consistent with our previous studies of the wild-type protein (*11*). From each fit, the populations of both monomer and dimer can be calculated at each radial distance, as shown in panels a−c of Figure 2 by the dashed and dotted lines, respectively. Under these experimental conditions, wild-type OMPLA (Figure 2a) exhibits a majority population of dimer, and the average apparent free energy of association from three independent experiments was found to be −8.18 ± 0.20 kcal/mol. H234A, shown in Figure 2b, has an apparent free energy of association of −8.86 ± 0.25 kcal/mol. Although this association is less than 1 kcal/mol stronger than that of the wild-type, it results in a noticeable increase in the dimer population from that of the wild-type under these conditions. In contrast, Figure 2c shows a marked decrease in dimer population from the wild-type as a consequence of the detrimental effect of the F109A substitution on dimer stability. For this sequence variant, the apparent free energy of association was −6.70 ± 0.12 kcal/mol, resulting in a loss of stability of 1.48 kcal/mol. We can more clearly discern trends in the data by focusing on how the equilibrium population of dimeric protein changes across a broad range of protein concentrations, as shown in Figure 3.

Of the 10 OMPLA variants, half did not experience any significant perturbations to dimer stability. Specifically, L32A (ranked first), F30A (fifth), L73A (14th), and the OSA control E25A (41st) all exhibited wild-type-like dimerization (Figure 3). Contrary to the loss of dimerization seen by Kingma et al. (*21*) as assessed by cross-linking, in our hands, Q94A also exhibited wild-type dimerization energetics, which agrees with previous work in our laboratory by Stanley et al. (*17*). While the energetic perturbations we observed are somewhat small, they can lead to large shifts in the population distributions of OMPLA, as shown in Figure 3. For example, at a total protein concentration of 1 μM, wild-type OMPLA and the five other wild-type-like variants are approximately 65% dimeric. In contrast, the dimeric population of L71A drops 35% compared to that of the wild-type, and F109A is less than 20% dimeric at this concentration. Interestingly, H234A (ranked second), S148A (third), and the control variant T112A (39th) dimerize more strongly than the wild-type. T112A shows a modest but statistically significant ($p < 0.05$) increase in stability (0.39 ± 0.19 kcal/mol), and both H234A and S148A exhibit a 0.7 ± 0.25 kcal/mol increase in dimer stability. Although this difference in the apparent free energy of association is slight in comparison to the detrimental variants, it results in an almost 20% increase in dimer population for S148A and H234A (Figure 3) above that of the wild-type at a protein concentration of 1 μM.

The Enzymatic Activities of Seven of Ten OMPLA Sequence Variants Are Consistent with Wild-Type-like Interface Architecture. Since interfacial packing changes had energetic consequences with respect to the free energy of dimerization that did not coincide with those anticipated from the OSA rankings, we used a functional assay to assess the structural integrity of the variants. The phospholipase activity of OMPLA requires precise interface architecture to maintain the substrate binding sites, the catalytic sites, and the calcium binding sites necessary for efficient activity. Therefore, specific activity can be used to determine whether major

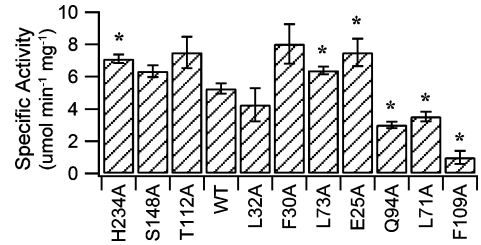

FIGURE 4: Specific activity of OMPLA interface packing variants. The specific activities shown here are measured using a DTNB colorimetric assay to monitor cleavage of the substrate HEPC. The activity of each variant was measured in 2.5 mM C14-SB micelles. The average activity and standard deviation were calculated on the basis of these data and are represented in the figure. The asterisks indicate a statistical difference from the wild-type value ($p < 0.05$) as determined by a Student's *t* test.

structural rearrangements are occurring on the dimer interface upon mutagenesis. To test this, we utilized a colorimetric assay developed by Stanley et al. to measure the specific activity of these OMPLA variants (*17*). Figure 4 shows the specific activities of the wild-type protein and the sequence variants. Seven of the ten sequence variants demonstrate wild-type-like or better specific activity. Q94A, L71A, and F109A exhibit statistically significant decreases in activity ($p < 0.05$). Of these, L71A and F109A also exhibited significant decreases in dimer stability from that of the wild-type. Dimerization is a fundamental regulator of and prerequisite for OMPLA enzyme activity because each monomer lacks complete binding sites. Thus, our data cannot distinguish between whether the L71A and F109A mutations cause perturbations that only disrupt dimer stability and subsequently show decreased activity or whether they cause perturbations that disrupt dimer stability and also alter important enzymatic architecture. Interestingly, Q94A also exhibits a decrease in activity but exhibits wild-type-like dimerization. Along these same lines, E25A and L73A also exhibit wild-type-like dimerization but increased enzymatic activity, suggesting that some residues may contribute to activity, although they may not contribute to dimerization.

Resistance to Thermal Denaturation Suggests Interfacial Packing Variants Are Not Significantly Destabilized. Seven of the ten variants were enzymatically competent, suggesting that the dimer interface of these variants did not undergo significant structural rearrangements. However, to further address whether the alanine substitutions affected the thermodynamic stability of the monomer, we used resistance to thermal denaturation as a qualitative measure of protein stability. A previous study focusing on the energetic consequences of polar mutations at the OMPLA interface suggested that substitutions at these sites could substantially reduce the resistance of the OMPLA monomer to thermal denaturation compared to that of the wild-type (*17*). We used this assay to interrogate whether the packing mutations we introduced in this study had similar affects. In this assay, proteins are heated to 80 °C for 10 min in the presence of SDS loading buffer. Folded OMPLA variants retain a compact structure on SDS−PAGE and separate from unfolded OMPLA variants, which migrate at their true molecular weight. All variants retained this characteristic heat modifiability. Densitometry analysis of SDS−PAGE allows determination of the relative population of unfolded and folded protein after thermal denaturation. Figure 5 compares

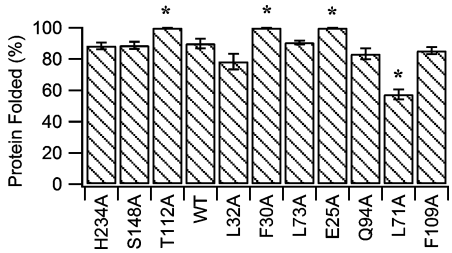

FIGURE 5: Thermal denaturation of interfacial packing variants. Aliquots of folded variants from specific activity samples were thermally denatured at 80 °C for 10 min in the presence of 0.5× SDS−PAGE loading buffer. The percentage that remained folded was determined by densitometry of SDS−PAGE analysis. The asterisks indicate a statistical difference from the wild-type value ($p < 0.05$) as determined by a Student's *t* test.

the percent of protein that remains folded for each variant after it has been heated for 10 min. Overall, interface packing variants were not more sensitive to thermal denaturation than the wild-type. Interestingly, three variants (F30A, E25A, and T112A) were actually statistically more resistant to thermal denaturation than wild-type OMPLA ($p < 0.05$). Only L71A exhibited a statistically significant loss of folded protein ($p < 0.05$), with only 60% remaining folded after this heat treatment.

DISCUSSION

No Correlation Was Found between Loss of Intermonomer Occluded Surface Area and Perturbations to the Apparent Free Energy of Association. van der Waals interactions had previously been shown to be strong determinants of stabilization of the lateral interactions of helices in predominantly α-helical membrane proteins (*7*−*10*). Faham and colleagues measured changes in thermodynamic stability via an equilibrium unfolding assay on 24 individual alanine substitutions on the B helix of the α-helical multipass membrane protein bacteriorhodopsin (bR) (*8*). The free energy change due to mutation was used for 20 of these sequence variants and was compared to the loss of buried surface area (BSA). The crystal structure of one sequence variant (P50A) was used to calculate the actual loss of BSA, and the changes in BSA for the remaining 19 sequence variants were calculated by computationally modeling the alanine substitution onto the wild-type bR crystal structure. By examining the energetic changes in protein stability with respect to the buried surface area values, Faham found a linear correlation of structure and energetics revealing that 38 Å^2 of buried surface area provides ∼1 kcal/mol in stability. Independent work using the GpA dimer utilized occluded surface area (OSA) to improve our understanding of this correlation. Occluded surface area is similar to buried surface area but allows for a more responsive analysis of packing interactions between buried residues and allows calculation of residue-specific values. Using OSA calculations, Doura et al. examined 23 variants at seven locations on the GpA dimer interface and suggested that each reduction of 26 Å^2 of favorable occluded surface area cost 1 kcal/mol of stability. These correlations between residue packing and stability are remarkably similar given the distinct differences in the tertiary structures of bR and GpA as well as the many differences in the experimental conditions for these two studies. These findings therefore suggested that the relationship between packing interactions and stability is inherent to the protein−protein interactions irrespective of the structural hierarchical context.

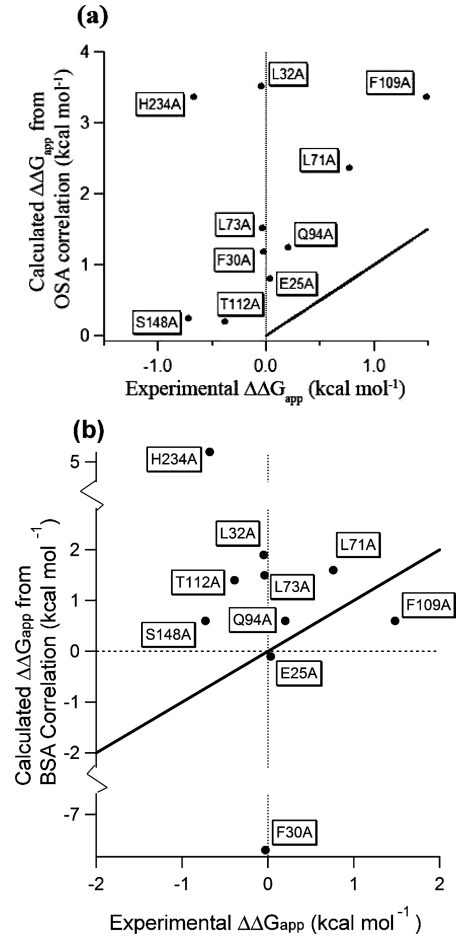

FIGURE 6: Comparison of experimental and calculated changes in the apparent free energy of association from (a) OSA and (b) BSA correlations. BSA and OSA of each variant were calculated as described. The expected loss of OSA or BSA is the difference between the wild-type value and that calculated for each variant. The calculated $\Delta\Delta G_{app}$ was then determined by multiplying the expected loss by (a) the correlation determined by Doura et al. of 0.039 kcal mol^{-1} lost per 1 Å^2 of OSA lost or (b) the correlation determined by Faham et al. of 1 kcal mol^{-1} lost per 38 Å^2 of lost BSA. The solid line indicates the agreement between the experimental $\Delta\Delta G_{app}$ and the value calculated using the previously established linear correlation. The points for each variant indicate the calculated $\Delta\Delta G_{app}$ based on the expected loss of BSA or OSA with respect to the experimental $\Delta\Delta G_{app}$ determined by SE-AUC analysis.

However, our investigation of OMPLA dimerization suggests that this linear correlation may not be universally applicable. Figure 6 shows the lack of correlation between OMPLA dimer stability and either calculated occluded (Figure 6a) or buried (Figure 6b) surface area. Irrespective of the surface area calculation used, the experimental data for OMPLA deviate strongly from the solid lines predicted by the helical studies.

Since all of these structure−energy correlations depend on the structural models used to calculate them, we used biochemical approaches to experimentally verify our computational models. Like the bR and GpA studies, the structural changes due to the introduction of the alanine mutations are anticipated to be only small rearrangements restricted to the local side chain environment. In GpA, the robust stability of a helix in a membrane was used to argue

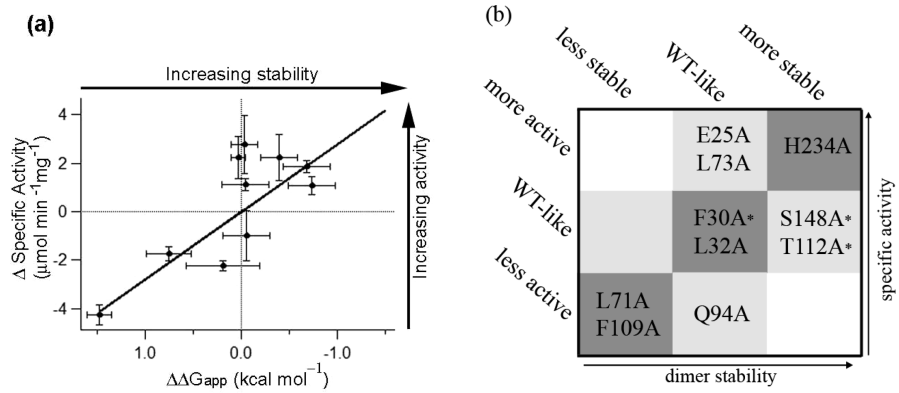

FIGURE 7: Comparison of changes in apparent free energy of association and changes in specific activity. (a) General trend in data. Each variant is represented by a point on the graph with *x* and *y* coordinates indicating the $\Delta\Delta G_{app}$ from that of the wild-type and the change in specific activity from that of the wild-type, respectively. The fitted line indicates a general trend in the data which shows that residues which result in an increase in dimerization stability will likely exhibit increased enzymatic activity and those which depress dimerization will most likely exhibit depressed activity. (b) Qualitative comparison of the change in the apparent free energy of association and the change in the specific activity for each variant. Each variant was classified in categories based on the results of the SE-AUC dimerization studies and the specific activity assay results. Variants are considered not wild-type-like if their deviation from wild-type behavior was statistically significant ($p < 0.05$) as determined by a Student's *t* test. Squares colored dark gray represent categories where specific activity and dimer stability correlate. White squares represent anomalous behavior where activity and stability are in complete disagreement. Residues labeled with asterisks have *p* values just above the established boundary.

that alanine substitutions would not lead to helix unfolding (*28*), and in bR, the retinal absorbance peak was used as an indicator of nativelike structure (*8*). Since OMPLA is an enzyme, we used specific activity to verify the integrity of the dimer, and we use resistance to thermal denaturation to detect any changes in the global monomer structure. Nine of ten variants exhibited wild-type-like sensitivity to thermal denaturation, suggesting that introduction of these packing defects did not cause dramatic changes in tertiary structure. Seven of the ten variants exhibit wild-type-like or better specific activity, indicating that the precise interface and active site architecture of the wild-type protein were preserved. Thus, we conclude that major structural rearrangements in response to these alanine substitutions are not the likely source of the disagreement between the OMPLA and both the GpA and the bR structure−energy correlations. Three OMPLA variants (F109A, L71A, and Q94A) do not exhibit wild-type behavior in the specific activity assay; however, excluding these variants does not improve the correlations with either buried surface area or occluded surface area. One caveat of this analysis is that our data have been evaluated using the crystal structures of both monomeric and dimeric OMPLA. These structures imply very little rearrangement upon oligomerization. Molecular dynamics simulations supported this overall finding but further suggested that the monomer may be more dynamic than the dimer (*29*). This result prompted Baaden et al. to hypothesize that the dynamic flexibility of OMPLA may be correlated with differences in catalytic activity, and it is plausible that the sequence variants in this study may also alter OMPLA dynamics. This cannot be addressed by our current methods; however, this intriguing possibility merits further investigation.

The Overall Mode of Activity Regulation Is Not Perturbed in the Interfacial Packing Variants. Although the energetic consequences of these packing variants cannot be correlated with loss of either occluded or buried surface area, the data do follow a trend that makes sense in the context OMPLA function. Since dimerization is necessary for enzymatic activity, we anticipated that the general trend of the dimer stability could predict the results of the activity assay: substitutions that increase dimer stability should lead to greater populations of dimer, which should also increase enzymatic activity in our assay. Figure 7a shows this is generally true. The correlation coefficient for a linear regression of the association free energies versus specific activities for all the variants equals 0.5979, confirming that dimerization propensities do modulate enzyme activity as expected. Figure 7b shows the generalized categories for the sequence variants and more broadly demonstrates that the fundamental regulatory mechanism encoded by OMPLA dimerization has not been perturbed. Changes in dimer stability and specific activities agree in five of the ten variants (H234A, L32A, F30A, L71A, and F109A), which occupy the dark gray squares along the diagonal. The two white squares in Figure 7b correspond to the positions expected for anomalous behavior and are empty, suggesting that the overall mode of regulating OMPLA activity is preserved in all sequence variants. The top left category, for example, would describe a variant that cannot stably form dimers but exhibits strong enzymatic activity: no such variant was observed. This is not surprising since substantial changes in the structural architecture of the substrate binding pocket and the catalytic site would be necessary to eliminate the native barriers to enzymatic competence in the monomer. Additionally, no variants with increased dimer stability exhibited significantly reduced activity (bottom right category).

While this overall mode of regulation is preserved, increased dimer stability is not enough to increase enzymatic activity. Both T112A and S148A exhibit wild-type activity despite statistically significant increases in dimer stability over that of the wild-type (represented by the center square). However, the activities of both of these variants had *p* values just above the established $p < 0.05$ boundary for significance (0.06 and 0.06), which might therefore represent some plasticity in the relationship between dimerization and activity.

The association free energies of this set of OMPLA sequence variants allow insight into the previously published results of Kingma and colleagues (*21*) in which calcium affinities of some OMPLA sequence variants were altered.

The crystal structure shows Leu32, Leu71, and Leu73 in the binding cleft (*12, 21*), and Kingma found that a leucine triple variant, L32A/L71A/L73A, exhibited an almost 600-fold decrease in calcium affinity from a micromolar wild-type value to a millimolar variant affinity. Since the calcium binding site must be created by a precise alignment of the two monomers, they concluded from this result that these residues were important for dimerization as well as maintaining the proper register of the two monomers with respect to calcium and substrate binding. Our study of the individual alanine substitutions at these sites shows a more precise profile of the resulting perturbations. While L32A and L73A both exhibit wild-type or better dimerization stability and enzymatic activity, L71A does not. Therefore, it is likely that the results observed by Kingma for L32A/L71A/L73A are solely ascribed to the single L71A mutation. Further, because the calcium affinity was diminished in Kingma's triple mutant, it is likely altered in the L71A packing variant as well. Kingma et al. showed wild-type calcium affinity varied by more than 500-fold depending on the substrate and detergent conditions. Using the conditions that best matched those used here, we estimate that at our experimental calcium concentrations, calcium would be bound to at least 75% of the protein. This may have influenced the dimerization and activity exhibited by L71A. However, the thermal denaturation sensitivity indicates that L71A does not have wild-type-like structural integrity, for which changes in calcium affinity cannot account. We postulate that the structure of L71A has an altered architecture relative to that of the wild-type, and the perturbations to dimerization and activity are reflections of these structural rearrangements.

In conclusion, our results improve our understanding of the intricate interactions that help maintain the monomer−dimer equilibrium responsible for dimer stability and enzymatic function in OMPLA; however, a more general explanation of the loss of contact area at the dimer interface does not apply for this protein. Since the correlation shown for α-helical membrane proteins (*7, 8*) cannot predict the observed perturbations to dimer stability in β-barrel membrane protein OMPLA, it appears that stability is mediated differently for this β-barrel membrane protein than it is for the α-helical interactions encoded by the GpA dimer and bR. An improved predictive model for how protein stability is mediated in membrane proteins is necessary, and further structural and thermodynamic studies will be required to realize this goal.

SUPPORTING INFORMATION AVAILABLE

Table 1 gives representative statistics for the SE-AUC fits of wild-type OMPLA and packing variants. One representative globally fit data set (three initial protein concentrations and three speeds) for the wild-type and each of the ten variants is given in this table. For each data set, raw SE-AUC data were fit to a single ideal as well as monomer, dimer, monomer−dimer, and monomer−trimer models to determine which best described the data. In each case, the data were best described by a monomer−dimer fit, which is illustrated by a low square root of variance value (SRV). The degrees of freedom (DoF) for each fit are also given as well as the sigma (σ) determined by the single ideal fit. In all cases, the calculated σ of the monomer is 1.4093. This material is available free of charge via the Internet at http://pubs.acs.org.

REFERENCES

1. Arbely, E., and Arkin, I. T. (2004) Experimental measurement of the strength of a Cα−H···O bond in a lipid bilayer. *J. Am. Chem. Soc. 126*, 5362–5363.
2. Engelman, D. M., Chen, Y., Chin, C. N., Curran, A. R., Dixon, A. M., Dupuy, A. D., Lee, A. S., Lehnert, U., Matthews, E. E., Reshetnyak, Y. K., Senes, A., and Popot, J. L. (2003) Membrane protein folding: Beyond the two stage model. *FEBS Lett. 555*, 122–125.
3. Hildebrand, P. W., Gunther, S., Goede, A., Forrest, L., Frommel, C., and Preissner, R. (2008) Hydrogen-bonding and packing features of membrane proteins: Functional implications. *Biophys. J. 94*, 1945–1953.
4. Mottamal, M., and Lazaridis, T. (2005) The contribution of Cα−H···O hydrogen bonds to membrane protein stability depends on the position of the amide. *Biochemistry 44*, 1607–1613.
5. Zhou, F. X., Cocco, M. J., Russ, W. P., Brunger, A. T., and Engelman, D. M. (2000) Interhelical hydrogen bonding drives strong interactions in membrane proteins. *Nat. Struct. Biol. 7*, 154–160.
6. Joh, N. H., Min, A., Faham, S., Whitelegge, J. P., Yang, D., Woods, V. L., and Bowie, J. U. (2008) Modest stabilization by most hydrogen-bonded side-chain interactions in membrane proteins. *Nature 453*, 1266–1270.
7. Doura, A., Kobus, F. J., Dubrovsky, L., Hibbard, E., and Fleming, K. G. (2004) Sequence context modulates the stability of a GxxxG-mediated transmembrane helix-helix dimer. *J. Mol. Biol. 341*, 991–998.
8. Faham, S., Yang, D., Bare, E., Yohannan, S., Whitelegge, J. P., and Bowie, J. U. (2004) Side-chain contributions to membrane protein structure and stability. *J. Mol. Biol. 335*, 297–305.
9. Fleming, K. G., Acherman, A. L., and Engelman, D. M. (1997) The effect of point mutations on the free energy of transmembrane α helix dimerization. *J. Mol. Biol. 272*, 266–275.
10. Fleming, K. G., and Engelman, D. M. (2001) Specificity in transmembrane helix-helix interactions can define a hierarchy of stability for sequence variants. *Proc. Natl. Acad. Sci. U.S.A. 98*, 14340–14344.
11. Stanley, A. M., Chuawong, P., Hendrickson, T. L., and Fleming, K. G. (2006) Energetics of outer membrane phospholipase A (OMPLA) dimerization. *J. Mol. Biol. 358*, 120–131.
12. Snijder, H., Ubarretxena-Belandia, I., Blaauw, M., Kalk, K. H., Verheij, H. M., Egmond, M. R., Dekker, N., and Dijkstra, B. W. (1999) Structural evidence for dimerization-regulated activation of an integral membrane phospholipase. *Nature 401*, 717–721.
13. Dekker, N., Tommassen, J., Lustig, A., Rosenbusch, J. P., and Verheij, H. M. (1997) Dimerization regulates the enzymatic activity of *Escherichia coli* outer membrane phospholipase A. *J. Biol. Chem. 272*, 3179–3184.
14. Connolly, M. (1993) The molecular surface package. *J. Mol. Graphics 11*, 139–141.
15. Horrevoets, A., Francke, C., Verheij, H. M., and de Haas, G. H. (1991) Activation of reconstituted *Escherichia coli* outer-membrane phospholipase A by membrane-perturbing peptides results in an increased reactivity towards the affinity label hexadecanesulfonyl fluoride. *Eur. J. Biochem. 198*, 255–261.
16. Horrevoets, A., Verheij, H. M., and de Haas, G. H. (1991) Inactivation of *Escherichia coli* outer-membrane phospholipase A by the affinity label hexadecanesulfonyl fluoride. Evidence for an active-site serine. *Eur. J. Biochem. 198*, 247–253.
17. Stanley, A. M., and Fleming, K. G. (2007) The role of a hydrogen bonding network in the transmembrane β-barrel OMPLA. *J. Mol. Biol. 370*, 912–924.
18. Stanley, A. M., Treubrodt, A. M., Chuawong, P., Hendrickson, T. L., and Fleming, K. G. (2007) Lipid chain selectivity by outer membrane phospholipase A. *J. Mol. Biol. 366*, 461–468.
19. Yphantis, D. (1964) Equilibrium ultracentrifugation of dilute solutions. *Biochemistry 3*, 297–317.
20. Pattabiraman, N., Ward, K. B., and Fleming, P. J. (1995) Occluded molecular surface: Analysis of protein packing. *J. Mol. Recognit. 8*, 334–344.
21. Kingma, R., and Egmond, M. R. (2002) Activation of a covalent outer membrane phospholipase A dimer. *Eur. J. Biochem. 269*, 2178–2185.

22. Doura, A. K., and Fleming, K. G. (2004) Complex interactions at the helix-helix interface stabilize the glycophorin A transmembrane dimer. *J. Mol. Biol. 343*, 1487–1497.
23. Ebie, A. Z., and Fleming, K. G. (2007) Dimerization of the erythropoietin receptor transmembrane domain in micelles. *J. Mol. Biol. 366*, 517–524.
24. Fleming, K. G., Ren, C. C., Doura, A. K., Eisley, M. E., Kobus, F. J., and Stanley, A. M. (2004) Thermodynamics of glycophorin A transmembrane helix dimerization in C14 betaine micelles. *Biophys. Chem. 108*, 43–49.
25. Kroch, A., and Fleming, K. G. (2006) Alternative interfaces may mediate homomeric and heteromeric assembly in the transmembrane domains of SNARE proteins. *J. Mol. Biol. 357*, 184–194.
26. Stanley, A. M., and Fleming, K. G. (2005) The transmembrane domains of ErbB receptors do not dimerize strongly in micelles. *J. Mol. Biol. 347*, 759–772.
27. Johnson, M., Correia, J. J., Yphantis, D. A., and Halvorson, H. R. (1981) Analysis of data from the analytical ultracentrifuge by nonlinear least-squares techniques. *Biophys. J. 36*, 575–588.
28. Popot, J. L., and Engelman, D. M. (1990) Membrane protein folding and oligomerization: The two-stage model. *Biochemistry 29*, 4031–4037.
29. Baaden, M., Meier, C., and Sansom, M. S. (2003) A molecular dynamics investigation of mono and dimeric states of the outer membrane enzyme OMPLA. *J. Mol. Biol. 331*, 177–189.

BI801436A